scientific reports

Check for updates

OPEN

# Diffuse pulmonary ossification and its association with cicatricial organising pneumonia in idiopathic and secondary forms

Yasuhiro Terasaki[1,2]✉, Yasuhiko Nishioka[3], Yusuke Kajimoto[2], Yuko Toyoda[4], Akira Hebisawa[5], Takeshi Johkoh[6], Ryoko Egashira[7], Takeshi Hisada[8], Masamichi Mineshita[9], Tomohisa Baba[10], Yuji Fujikura[11], Motoyasu Kato[12], Kazuya Ichikado[13], Yoshikazu Inoue[14], Shinyu Izumi[15], Yoshinori Hasegawa[16], Tomohiro Handa[17], Koko Hidaka[18], Shu Hisata[19], Chisato Honjo[20], Takumi Kishimoto[21], Masaki Okamoto[22], Mari Yamasue[23], Mika Terasaki[2] & Takafumi Suda[24]

**Diffuse pulmonary ossification (DiPO) is characterised by widespread ectopic bone formation in the lungs. Idiopathic DiPO (I-DiPO) poses significant diagnostic challenges and its ossification mechanism remains unclear. Cicatricial organising pneumonia (CiOP) lesions form fibrous nodules without damaging lung structure. We investigated the histopathological features of I-DiPO, focusing on the surrounding fibrosis, and compared them with those of secondary DiPO (S-DiPO). An analysis was conducted using data from a nationwide DiPO survey in Japan. The dataset included clinical, radiological, and histopathological data of patients with suspected I-DiPO. The specific patterns of ossification and fibrotic findings such as CiOP, organising pneumonia (OP), and subpleural fibrosis were identified. Eighteen and seven patients were classified as having I-DiPO and S-DiPO, respectively. I-DiPO affects younger patients, progresses slowly, commonly occurs in the lower lungs, and has a lower mortality rate. S-DiPO affects older patients, presents with widespread lung lesions, and has a higher mortality rate. CiOP lesions were found in direct continuity with or near ossified lesions in 61.1% and 71.4% of patients with I-DiPO and S-DiPO, respectively. OP, CiOP, and ossified lesions often observed in the same locations in S-DiPO. DiPO has a unique pathogenesis, with an ossification transition occurring via the CiOP lesions. These findings provide valuable insights for future diagnostic approaches and management strategies for this condition.**

**Keywords** Diffuse pulmonary ossification, Cicatricial organising pneumonia, Dendritic pulmonary ossification, Idiopathic diffuse pulmonary ossification, Secondary diffuse pulmonary ossification

[1]Division of Pathology, Nippon Medical School Hospital, 1-1-5 Sendagi, Bunkyo-Ku, Tokyo 113-8603, Japan. [2]Department of Analytic Human Pathology, Nippon Medical School, 1-25-1 Nezu, Bunkyo-Ku, Tokyo 113-0031, Japan. [3]Department of Respiratory Medicine and Rheumatology, Graduate School of Biomedical Sciences, Tokushima University, 3-18-15 Kuramoto-Cho, Tokushima 770- 8503, Japan. [4]Department of Internal Medicine, Japanese Red Cross Kochi Hospital, 1-4-63-11, Hadnaminami-Machi, Kochi 780-8562, Japan. [5]Division of Clinical Pathology, NHO Tokyo National Hospital, 3-1-1 Takeoka, Kiyose, Tokyo 204-8585, Japan. [6]Department of Radiology, Kansai Rosai Hospital, 3-1-69 Inabaso, Amagasaki, Hyogo 660-8511, Japan. [7]Department of Radiology, Faculty of Medicine, Saga University, 5-1-1 Nabeshima, Saga 849-8501, Japan. [8]Department of Respiratory Medicine, Gunma University Graduate School of Medicine, 3-39-22 Showa Machi, Maebashi 371-8514, Japan. [9]Department of Respiratory Medicine, St. Marianna University School of Medicine, 2-16-1 Sugao, Miyamae-Ku, Kawasaki 216-8511, Japan. [10]Department of Respiratory Medicine, Kanagawa Cardiovascular and Respiratory Centre, 6-16-1 Tomioka-Higashi, Kanazawa-Ku, Yokohama 236-0051, Japan. [11]Division of Infectious Diseases and Respiratory Medicine, Department of Internal Medicine, National Defense Medical College, 3-2 Namiki, Tokorozawa, Saitama 359- 8513, Japan. [12]Department of Respiratory Medicine, Juntendo University Graduate School of Medicine, 2-1-1 Hongo, Bunkyo-Ku, Tokyo 113-8421, Japan. [13]Department of Respiratory Medicine, Saiseikai Kumamoto Hospital, 5-3-1 Chikami, Minami-Ku, Kumamoto 861-4193, Japan. [14]Clinical Research Center, NHO Kinki Chuo Chest Medical Center, 1180 Nagasonecho, Kita-Ku, Sakai 591-8555, Japan. [15]Department of Respiratory Medicine, National Center for Global Health and Medicine, 1-21-1 Toyama, Shinjuku-Ku, Tokyo 162-8655, Japan. [16]Department

of Respiratory Medicine, Osaka Saiseikai Nakatsu Hospital, 2-10-39 Shibata, Kita-Ku, Osaka 530-0012, Japan. [17]Department of Advanced Medicine for Respiratory Failure, Graduate School of Medicine, Kyoto University, 54 Shogoinkawahara-Cho, Sakyo-Ku, Kyoto 6068507, Japan. [18]Department of Respiratory Medicine, National Hospital Organization Kokura Medical Center, 10-1 Harugaoka, Kokuraminami-Ku, Kitakyushu, Fukuoka 802-8533, Japan. [19]Division of Pulmonary Medicine, Jichi Medical University, 3311-1 Yakushiji, Shimotsuke, Tochigi 329-0498, Japan. [20]Department of Respiratory Medicine, University of Fukui Hospital, 23-3 Matsuokashimoaizuki, Eiheiji, Yoshida, Fukui 910-1193, Japan. [21]Department of Medicine, Okayama Rosai Hospital, 1-10-25 Chikkomidorimachi, Minami-Ku, Okayama 702-8055, Japan. [22]Division of Respirology, Neurology, and Rheumatology, Department of Internal Medicine, Kurume University School of Medicine, 67 Asahimachi, Kurume 830-0011, Japan. [23]Department of Respiratory Medicine and Infectious Diseases, Oita University Faculty of Medicine, 1-1 Idaigaoka, Hasama-Machi, Yufu 879-5593, Japan. [24]Second Division, Department of Internal Medicine, Hamamatsu University School of Medicine, 1-20-1 Handayama, Chuou-Ku, Hamamatsu 431-3192, Japan. ✉email: terasaki@nms.ac.jp

Diffuse pulmonary ossification (DiPO) is characterised by widespread ectopic bone formation in the lung tissue[1,2]. Histopathologically, DiPO is classified as nodular or dendriform pulmonary ossification[2–4] and is sometimes associated with underlying diseases, such as pulmonary diseases (including interstitial pneumonia [IP], chronic obstructive pulmonary disease, aspiration pneumonia, and acute respiratory distress syndrome [ARDS]), cardiac diseases (including congestive heart failure, mitral stenosis [MiS], and atrial fibrillation [Af] with chronic pulmonary venous congestion), endocrine diseases, and malignancies[4–8]. However, case reports of idiopathic DiPO (I-DiPO) with no apparent underlying disease have been published. I-DiPO is often asymptomatic, making it a challenging condition to diagnose. Recent advances in diagnostic imaging have identified characteristic chest computed tomography (CT) findings in several patients with I-DiPO, including diffuse calcified branching structures in bilateral lung fields. Consequently, the reported number of patients with I-DiPO has increased[9].

A comprehensive nationwide study on idiopathic dendriform pulmonary ossification was conducted between 2017 and 2019 in Japan[10], detailing its onset, clinical progression, radiological and histopathological characteristics, and potential prognostic factors such as the serum Krebs von den Lungen-6 level. Our findings highlight the need for increased awareness regarding idiopathic dendriform pulmonary ossification, which often develops asymptomatically in younger, predominantly male patients, progresses slowly, and frequently affects pulmonary function. Some patients develop pneumothorax[11,12] and severe progressive respiratory failure due to the ossification of the entire lung[13,14]. However, the mechanism by which ossification occurs, including in secondary DiPO (S-DiPO), remains unclear, and knowledge of I-DiPO is limited[1,15].

Cicatricial organising pneumonia (CiOP) lesions are characterised by intraluminal collagen deposition within a background of classic loose fibromyxoid organising pneumonia (OP). These lesions are occasionally accompanied by the formation of peculiar fibrous nodules or dense fibrotic linear bands, without significant destruction of the lung structure. Ossified lesions were reported as one of the characteristic findings in a previous case series of 'CiOP', in which interstitial lung disease was suspected with notable CiOP lesions on lung biopsies with frequencies ranging from 30 to 55%[16–18]. These findings highlight the potential involvement of ossification in the pathogenesis of CiOP, suggesting its relevance in understanding the disease spectrum. CiOP with dendriform ossification is an unusual cause of recurrent pneumothorax[19].

In this study, we primarily analysed the pathological features of I-DiPO, focusing on the fibrosis surrounding the ossification. To improve our understanding, we compared several patients with S-DiPO.

## Materials and methods

### Study design

This was a secondary survey of data from a retrospective nationwide survey of patients with I-DiPO conducted between 2017 and 2019 as part of the Research Project of the Study Group on Diffuse Pulmonary Disorders, Scientific Research/Research on Intractable Diseases in Japan[10]. Data on patients with DiPO were collected through a systematic survey of clinical, radiological, and histopathological data from facilities that managed patients with suspected I-DiPO who agreed to participate in the survey. In this study, rigorous inclusion and exclusion criteria were established, including the exclusion of secondary factors associated with autoimmune diseases. These criteria are detailed in the supplemental materials of the primary manuscript (Online Supplemental Table S1 and the Primary Survey Implementation Plan, Participants Section, see reference). Two respiratory physicians, two radiologists, and two histopathologists independently reviewed the clinical, radiological, and histopathological data; patients suspected of having other diseases or S-DiPO were excluded. The remaining patients were diagnosed as having I-DiPO. This study was conducted in accordance with the principles of the Declaration of Helsinki and approved by the Institutional Ethics Committee of Nippon Medical School (approval number: 0-2021-033).

### Radiological analyses

Chest radiography and high-resolution CT (HRCT) images were evaluated by two thoracic radiologists (J. T. and Y. E.) to determine the extent and distribution of calcified lesions and other related findings. The evaluated parameters included ossification (fine calcified nodules, calcified short lines, and calcified branching structures), fine nodules, short lines, branching structures, and fibrotic findings around the ossification or subpleural area (interlobular septal thickening, thickening of bronchovascular bundles, pleural thickening or irregularity, non-septal linear opacity, subpleural curvilinear shadow/line, cysts, ground-glass attenuation, and consolidation). The extent of the parenchymal findings was graded on a scale of 0–3: grade 0 (G0), none; grade 1 (G1), < 10%; grade 2 (G2), 10–30%; grade 3 (G3), 30–50%; and grade 4 (G4), > 50% of the lung field. Serial changes in the HRCT findings were also examined at the time of diagnosis and at the latest follow-up, when available.

### Histopathological analyses

All histopathological samples were evaluated using haematoxylin–eosin, Elastica Masson-Goldner, and Elastica van Gieson staining. Except for three patients with secondary DiPO who were autopsied (Patients 9, 12, and 31), all specimens were obtained via video-assisted thoracoscopic surgery. Each sample was examined on two slides. In addition to the screening phase for DiPO, two pulmonary histopathologists (Y. T. and A. H.) evaluated the histopathological features of diffuse ossified lesions based on the following parameters: ossification (number of ossified lesions per slide, maximum size, and bone marrow component) and fibrotic findings around the ossification or subpleural area. Each parameter was graded from 0 to 3. Diffuse ossified lesions were categorised into dendriform (a branching or tree-like pattern reminiscent of dendritic structures), nodular (a nodular pattern), or mixed (a combination of both) types, based on the pattern of the ectopic bone. The maximum size (diameter) of ossification was graded as follows: grade 0 (G0), 0–0.9 mm; grade 1 (G1), 1.0–1.9 mm; grade 2 (G2), 2.0–4.9 mm; and grade 3 (G3), ≥ 5 mm. The bone marrow component, fibrotic findings around the ossification, CiOP lesions, OP, and subpleural fibrosis as background IP were graded as follows: grade 0 (G0), none (not found by searching); grade 1 (G1), mild (only a few were found by searching); grade 2 (G2), moderate (often found by searching); and grade 3 (G3), severe (noticeable) (Supplementary Fig. 1 and Supplementary Text 1).

For pulmonary radiology and histopathology, all patients were independently and blindly evaluated to determine the pathological parameters according to the grade. In cases in which grade evaluation differed, the two radiologists or pathologists met to discuss the grade until a consensus was reached.

### Statistical analysis

To compare the clinical, radiological, and histopathological features of I-DiPO and S-DiPO, the Mann–Whitney U-test was used to analyse age, while Fisher's exact test was used to analyse sex, smoking status, laboratory data, lung function test, deterioration of pulmonary ossification on HRCT, survival rate, diffuse random distribution type, dendriform type, and other radiological or histopathological parameters as a ratio of higher grades (number of patients with G2, G3, or G4/number of all graded patients). Only patients with S-DiPO and Af were further compared with those with I-DiPO, in terms of ossification characteristics, such as morphological type, maximum size, and bone marrow components. Statistical significance was set at a two-tailed P value of $< 0.05$, while a two-tailed P value of $< 0.1$ was considered significant. Statistical analyses were performed using the GraphPad Prism 5 software (GraphPad Software, San Diego, CA, USA).

## Results

### Selection of patients with DiPO

The data from 39 patients were initially available for analysis with the assistance of the collaborators. One patient with pulmonary osteochondroma and 13 patients with unavailable histopathological specimens or insufficient histopathological specimens for evaluation (e.g., lung tissue obtained from transbronchial lung biopsy) were excluded.

Based on clinical, radiological, and histopathological reviews, 25 patients were diagnosed with DiPO. Of these, seven were diagnosed with S-DiPO, including three with IP (Patients 7, 12, and 36), two with Af and IP (Patients 24 and 31), one with Af and ARDS (Patient 9), and one with an background of MiS (Patient 27) (Table 1). The remaining 18 patients were diagnosed with I-DiPO (Fig. 1). The classification and diagnosis of IP in patients with S-DiPO was established based on the 2013 International Multidisciplinary Consensus Classification of Idiopathic Interstitial Pneumonias, published by the American Thoracic Society and the European Respiratory Society in the American Journal of Respiratory and Critical Care Medicine[20].

Of the 18 patients with I-DiPO and seven with S-DiPO, 14 (77.8%) and six (85.71%) were males, respectively. The mean ages at I-DiPO and S-DiPO diagnoses were 37.8 years and 67.8 years, respectively. Patients in the I-DiPO group were significantly younger than those in the S-DiPO group. Sixteen patients (88.9%) with I-DiPO and five (71.4%) with S-DiPO were never smokers. Alkaline phosphatase, corrected calcium, and inorganic phosphorus levels were not significantly different between the I-DiPO and S-DiPO groups. There were no patients with a clear background of autoimmune disease in either the I-DiPO or S-DiPO group. No significant differences were observed in the pulmonary function test results (% forced vital capacity and % forced expiratory volume in one second) between the two groups. Two patients (11.1%) in the I-DiPO group had a familial form, but there were none in the S-DiPO group. Of the 18 patients with I-DiPO, 14 (77.8%) were diagnosed at a medical checkup without any symptoms, while four (22.2%) were diagnosed due to respiratory symptoms, including cough, dyspnoea on exertion, and sputum. HRCT was performed in patients with DiPO, the images of which were available at two time points with a mean interval of 4.73 years (0.11–17.2 years). Thirteen (72.2%) patients with I-DiPO showed progression of ossified lesions on CT, including mild lesions. Two patients with I-DiPO were on the brain death transplant waiting list. Three of seven patients with S-DiPO died, including two diagnosed post-mortem, while no fatalities were observed in patients with I-DiPO. Based on the autopsy results, the causes of death were bacterial pneumonia with heart failure (Patient 9), acute exacerbation of IP with infection (Patient 12), and respiratory failure with progression of IP (Patient 31). I-DiPO showed a slow but progressive decline in pulmonary function, whereas longitudinal data for S-DiPO were limited due to fatal outcomes (Table 1 and Supplementary Table S5). Of the 25 patients, the details of nine have been reported in various journals[9,12,13,21–25].

### Radiological features of I-DiPO

Typical chest radiographs and HRCT findings of the three patients with I-DiPO are shown in Fig. 2 (a and b, Patient 3; c and d, Patient 10; and e and f, Patient 28). Chest radiography revealed bilateral linear, reticular, and nodular shadows mainly distributed in the lower lung fields. HRCT revealed linear opacities and

| | Idiopathic (N = 18) | Secondary (N = 7) | Test result P value |
|---|---|---|---|
| Sex (M:F) | 14:4 | 6:1 | |
| Male (M) | 14 (77.8%) | 6 (85.71%) | NS |
| Female (F) | 4 (22.2%) | 1 (14.29%) | |
| Mean age at diagnosis of DiPO | 37.8 (years) | 67.8 (years) | < 0.05 |
| Smoking status (N:F) | 16:2 | 5:2 | |
| Never (N) | 16 (88.9%) | 5 (71.4%) | NS |
| Former (F) | 2 (11.1%) | 2 (28.6%) | |
| Laboratory data | | | |
| ALP (U/L: 80–260) | 218.31 (N = 16) | 259.00 (N = 6) | NS |
| Corrected Ca (mg/dL: 8.4–10.4) | 9.43 (N = 16) | 9.32 (N = 5) | NS |
| P (mg/dL: 2.5–4.5) | 3.20 (N = 13) | 3.60 (N = 1) | NS |
| Lung function test | | | |
| %FVC | 86.83 (N = 18) | 90.45 (N = 4) | NS |
| $\%FEV_1$ | 80.95 (N = 18) | 87.75 (N = 4) | NS |
| Family history | 2 (10%) | 0 | |
| Deterioration of pulmonary ossification on HRCT | (N = 18) | (N = 4) | |
| Stable | 2 (11.1%) | 1 (14.29%) | NS |
| Progression | 13 (72.2%) | 1 (14.29%) | |
| Unknown | 3 (16.7%) | 5 (71.4%) | |
| Survival | (N = 18) | (N = 4) | |
| Alive | 16 (88.9%) | 3 (42.9%) | < 0.05 |
| Dead | 0 | 3 (42.9%) | |
| Unknown | 2 (11.1%) | 1 (14.2%) | |
| Underlying diseases | | (N = 4) | |
| Interstitial pneumonia | | 5 (71.43%) | |
| Atrial fibrillation | | 3 (42.86%) | |
| Acute respiratory distress syndrome | | 1 (14.30%) | |
| Mitral stenosis | | 1 (14.30%) | |

**Table 1**. Clinical characteristics of patients with I-DiPO and S-DiPO. *I-DiPO,* idiopathic diffuse pulmonary ossification; *S-DiPO,* secondary diffuse pulmonary ossification; *NS*, not significant; *ALP,* alkaline phosphatas; *Ca,* corrected calcium; *P,* inorganic phosphorus; *FVC,* forced vital capacity; $FEV_1$, forced expiratory volume in one second. Values represent the number of cases. Numbers in parentheses ( ) represent the percentages of patients in each group. Student's t-test or Mann–Whitney U test was used to analyse age, while Fisher's exact test was used to analyse sex and smoking status.

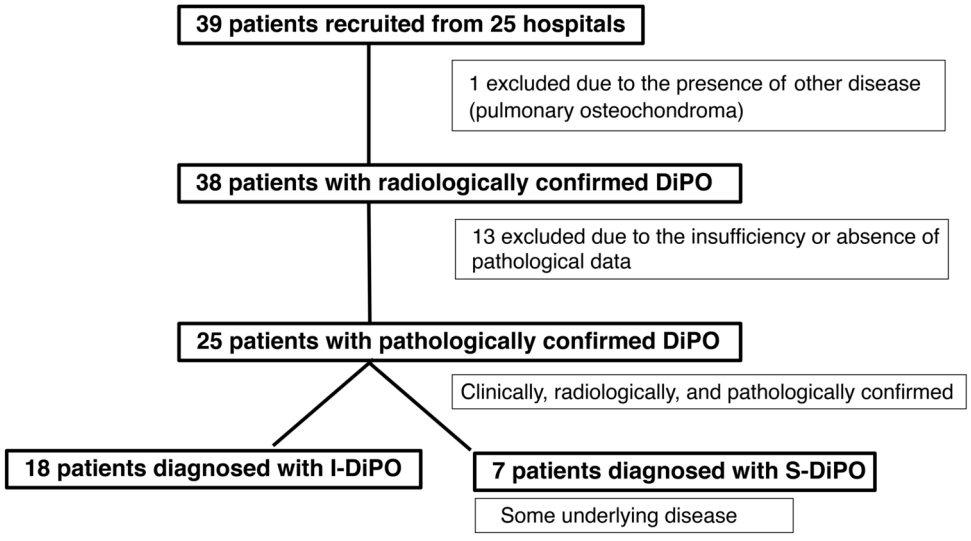


**Fig. 1**. Flow chart showing the selection of patients with I-DiPO and S-DiPO. *I-DiPO* idiopathic diffuse pulmonary ossification, *S-DiPO* secondary diffuse pulmonary ossification.

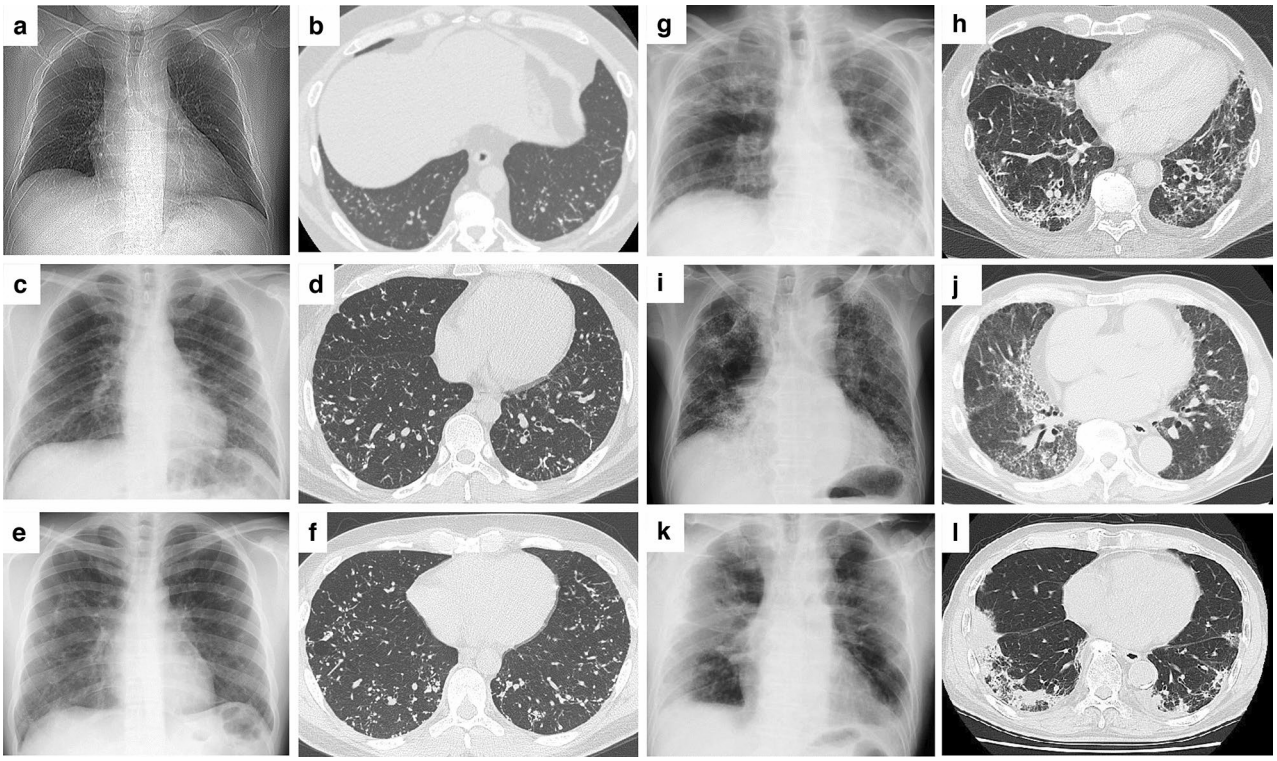


**Fig. 2**. Radiological findings of lung lesions detected in three patients with I-DiPO and three patients with S-DiPO. Three patients with I-DiPO had low (calcified total score = 3; **a**, **b**, Patient 3), medium (score = 4; **c**, **d**, Patient 10), and high (score = 5; **e**, **f**, Patient 28) levels of calcified lesions. The calcified total score represents the sum of grades from three assessment items for calcified lesions: fine calcified nodules, calcified short lines, and calcified branching structures. Three patients with S-DiPO had ossified lesions associated with IP (**g**, **h**, Patient 12) and ossified lesions associated with Af and IP (**i**, **j**, Patient 31; **k**, **l**, Patient 24). (**a**, **c**, **e**, **g**, **i**, **k**) Chest radiographs; (**b**, **d**, **f**, **h**, **j**, **l**) computed tomography horizontal sections under lung window settings. *Af* Atrial fibrillation, *I-DiPO* idiopathic diffuse pulmonary ossification, *IP* interstitial pneumonia, *S-DiPO* secondary diffuse pulmonary ossification.

nodules with calcified lesions predominantly in the lower lung fields. To further clarify the HRCT findings, systematic and semiquantitative evaluations were performed independently by two radiologists (Fig. 2, Table 2, and Supplementary Table S1). Regarding the craniocaudal distribution of the lung lesions, a lower lung field predominance was found in 15/18 (83.3%) patients with I-DiPO, whereas a diffuse random distribution was less common (3/18, 16.7%). In terms of axial distribution, diffuse, peribroncho-vascular, and peripheral areas were observed in 14/18 (77.8%), 3/18 (16.7%), and 1/18 (5.6%) patients with I-DiPO, respectively. All patients with I-DiPO had fine calcified nodules, calcified short lines, and calcified branching structures. Of the patients, 11/18 (61.1%) had fine calcified nodules, and calcified branching structures spread to 10–30% of the lung field as grade 2 (G2). Interstitial lung changes were observed, such as thick broncho-vascular bundles, thick or irregular pleura, and non-septal linear opacities. No pulmonary curvilinear shadows or lines, ground-glass attenuation, or consolidation were observed (Fig. 2, Table 2, and Supplementary Table S1).

## Radiological features of S-DiPO

The typical chest radiography and HRCT findings of the three patients with S-DiPO are shown in Fig. 2 (g–h, Patient 12; i–j, Patient 31; and k–l, Patient 24, respectively). With regard to the distribution of lung lesions in the craniocaudal direction, a diffuse random distribution was more frequent (5/7, 71.4%), whereas lower lung field predominance was less common in the S-DiPO group (2/7, 28.6%). The opposite trend was observed in the I-DiPO group (diffuse random, 3/18, 16.7%; lower-field predominance, 15/18, 83.3%) (Fig. 2, Table 2, and Supplementary Table S2).

Fine calcified nodules and short calcified lines, similar to those in the I-DiPO group, were observed. However, higher grades of calcified branching structures were seen in the I-DiPO group (11/18, 61.1%) than in the S-DiPO group (1/7, 14.3%) (Fig. 2 and Table 2). In contrast, six of the seven patients with S-DiPO had a background of IP (three with IP alone, two with AF and IP, and one with AF and ARDS). Higher prevalences of radiological fibrotic findings, such as fine nodules (5/7, 71.4%), ground-glass attenuation (5/7, 71.4%), and non-septate linear opacities (3/7, 42.9%), were observed in the S-DiPO group than in the I-DiPO group (2/18, 11.1%; 0/18, 0%; and 0/18, 0%). The radiological characteristics of the patients with I-DiPO and S-DiPO are summarised in Table 2 and Supplementary Tables S1 and S2, respectively.

| Distribution/ craniocaudal | Underlying diseases | Upper/middle field predominance | Lower field predominance | Diffuse random | No. of lower field predominance type/all types | % | F test P value |
|---|---|---|---|---|---|---|---|
| | Idiopathic | 0 | 15 | 3 | 15/18 | 83.3 | < 0.05 |
| | Secondary | 0 | 2 | 5 | 2/7 | 28.6 | |
| **Distribution/axial** | | **Peripheral** | **Peribroncho-vascular** | **Diffuse** | **No. of diffuse type/all types** | | |
| | Idiopathic | 1 | 3 | 14 | 14/18 | 77.7 | NS |
| | Secondary | 0 | 0 | 7 | 7/7 | 100 | |

| Radiological patterns | Underlying diseases | No. of G0 | No. of G1 | No. of G2 | No. of G3 + 4 | No. of G2 + 3 + 4/all grades | % | F test P value |
|---|---|---|---|---|---|---|---|---|
| Fine calcified nodule | Idiopathic | 0 | 7 | 11 | 0 | 11/18 | 61.1 | 0.202 |
| | Secondary | 0 | 5 | 2 | 0 | 2/7 | 28.6 | |
| Calcified short lines | Idiopathic | 0 | 18 | 0 | 0 | 0/18 | 0 | NS |
| | Secondary | 1 | 6 | 0 | 0 | 0/7 | 0 | |
| Calcified branching structures | Idiopathic | 0 | 7 | 11 | 0 | 11/18 | 61.1 | < 0.05 |
| | Secondary | 1 | 5 | 1 | 0 | 1/7 | 14.3 | |
| Fine nodules | Idiopathic | 0 | 16 | 2 | 0 | 2/18 | 11.1 | < 0.01 |
| | Secondary | 0 | 2 | 5 | 0 | 5/7 | 71.4 | |
| Short lines | Idiopathic | 1 | 17 | 0 | 0 | 0/18 | 0 | NS |
| | Secondary | 1 | 4 | 2 | 0 | 2/7 | 28.6 | |
| Branching structures | Idiopathic | 0 | 17 | 1 | 0 | 1/18 | 5.6 | NS |
| | Secondary | 1 | 4 | 2 | 0 | 2/7 | 28.6 | |
| Interlobular septal thickening | Idiopathic | 4 | 14 | 0 | 0 | 0/18 | 0 | NS |
| | Secondary | 1 | 4 | 1 | 1 | 2/7 | 28.6 | |
| Pleural thickening or irregularity | Idiopathic | 9 | 9 | 0 | 0 | 0/18 | 0 | NS |
| | Secondary | 3 | 3 | 0 | 1 | 1/7 | 14.3 | |
| Non-septal linear opacity | Idiopathic | 11 | 7 | 0 | 0 | 0/18 | 0 | < 0.05 |
| | Secondary | 3 | 1 | 2 | 1 | 3/7 | 42.9 | |
| Ground-glass attenuation | Idiopathic | 18 | 0 | 0 | 0 | 0/18 | 0 | < 0.01 |
| | Secondary | 2 | 0 | 2 | 3 | 5/7 | 71.4 | |
| Consolidation | Idiopathic | 18 | 0 | 0 | 0 | 0/18 | 0 | NS |
| | Secondary | 2 | 3 | 2 | 0 | 2/7 | 28.6 | |

**Table 2**. Comparison of the radiological characteristics between the I-DiPO and S-DiPO groups by distribution type and grading. *I-DiPO,* idiopathic diffuse pulmonary ossification; *S-DiPO,* secondary diffuse pulmonary ossification; *NS,* not significant; *F test,* Fisher's exact test. Values indicate the number of cases. G0: none, G1: < 10%, G2: 10–30%, G3: 30–50%, and G4: > 50% of the lung fields. To compare the radiological features of I-DiPO and S-DiPO, Fisher's exact test was used to evaluate the diffuse-random type, and all other radiological parameters were expressed as a ratio of higher grades (number of patients with G2, G3, and G4/ number of patients in all grades).

## Histopathological characteristics of I-DiPO

The typical histopathological findings in one patient with I-DiPO are shown in Fig. 3 (Patient 19). All patients with I-DiPO had predominantly dendriform ossified lesions with foci containing fat components or bone marrow (Fig. 3a–c,e; dendritic type, maximum size-G2, bone marrow-G3). Most cases had dendritic lesions (13 patients), while five patients had mixed-type lesions (Table 3 and Supplementary Table S3). A few ossified lesions were > 5 mm in size, while the maximum size of the ossified lesions was 1.0–6.0 mm (Table 3 and Supplementary Table S3). This bone tissue often proliferates while avoiding existing structures, such as bronchi and blood vessels. However, fibrous continuity was observed in the bronchial wall (Fig. 3b,c,e) and alveolar wall structures were present in the ossification foci (Fig. 3d). Therefore, ossification was continuously distributed from the interstitial areas of the bronchi, vessels, and pleura, to the surrounding air spaces.

CiOP of varying severity, with more hyalinising fibrous bands or nodules, was observed in direct continuity with or in the vicinity of the ossified lesions in 11 of the 18 patients with I-DiPO, as shown in Fig. 3e,f (Patient 19; CiOP-G1), Fig. 4a,b (Patient 37; CiOP-G2, maximum size-G1, bone marrow-G1), Fig. 4c–e (Patient 28; CiOP-G2, maximum size-G1, bone marrow-G2), and Fig. 4f–h (Patient 14; CiOP-G2, maximum size-G3, bone marrow-G3). However, this was unclear or scarcely detectable in seven patients (Patients 1, 4, 6, 8, 29, 30, and 35) (Table 3 and Supplementary Table S3).

In patients with CiOP lesions, osteoblastic cells embedded in ossified extracellular matrix were occasionally observed (Fig. 4d,e). CiOP and ossified lesions were visualised in the alveolar spaces by elastic fibre staining (Fig. 4f–h). In contrast, among patients with I-DiPO, high-grade subpleural fibrosis or OP was not observed (Table 3 and Supplementary Table S3).

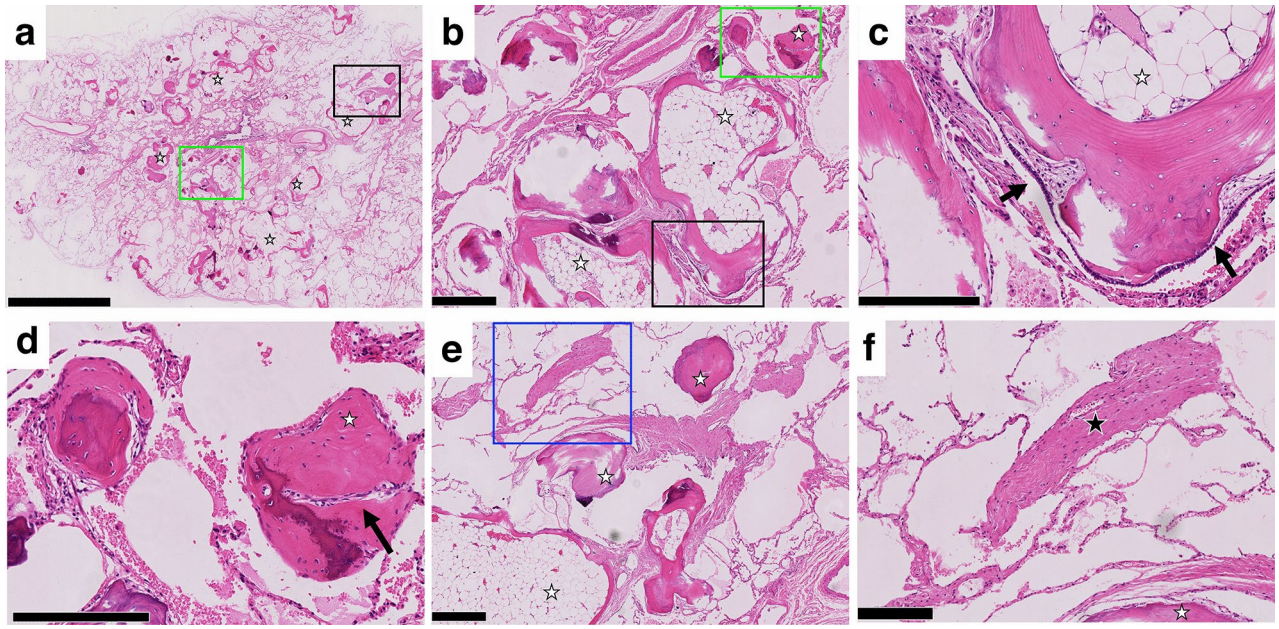


**Fig. 3**. Pathological findings of lung lesions from patients with I-DiPO. (**a**) Low-power view of a specimen obtained from a patient with I-DiPO (Patient 19). Multiple bone foci (white stars, dendritic type, maximum size-G2) in a branching pattern or randomly located. Haematoxylin and eosin staining. (**b**) Multiple ossified lesions (white stars) of various sizes with or without bone marrow components. High-magnification view of the green rectangle in (**a**). (**c**) An ossified lesion with bone marrow and fat components (white star, bone marrow-G3) in the bronchial wall. High-magnification views of the area within the black rectangle in (**b**) and the black arrows in (**c**) indicate the bronchial epithelium. (**d**) Alveolar wall structures are observed within the ossification lesions (white stars). High-magnification view of the green rectangle in (**b**). The black arrow in (**d**) indicates the alveolar wall. (**e**) Multiple ossified lesions (white stars) of varying sizes. High-magnification view of the area is indicated by the black rectangle in (**a**). (**f**) CiOP lesions as dense fibrous bands (black star, CiOP-G1) observed in the vicinity of the ossifying lesions (white stars). High-magnification view of the area is indicated by the blue rectangle in (**e**). Scale bars: 5 mm (**a**), 0.5 mm (**b**, **e**), and 0.25 mm (**c**, **d**, **f**). *CiOP* cicatricial organising pneumonia, *G* grade, *I-DiPO* idiopathic diffuse pulmonary ossification, *S-DiPO* secondary diffuse pulmonary ossification.

## Histopathological characteristics of S-DiPO

Of the seven patients with S-DiPO, two had the nodular type (Patients 9 and 31), three had the dendritic type (Patients 24, 27, and 36), and two had a mixed histological type (Patients 7 and 12) (Table 3 and Supplementary Table S4). Among the seven patients with S-DiPO, three (43%; Patients 7, 12, and 24) had high grades of OP as shown in Fig. 5a,b (Patient 7; OP-G3, maximum size-G2, bone marrow-G3) and Fig. 5d,e (Patient 12; mixed type, OP-G3, maximum size-G3, bone marrow-G1) and five (71%; Patients 9, 12, 31, 24, and 36) had high grades of subpleural fibrosis (Fig. 5c, Patient 24; subpleural fibrosis-G3, maximum size-G1, bone marrow-G0). Given the Given the IP background in these S-DiPO patients, the findings of OP and subpleural fibrosis in patients with S-DiPO were expected along with ossified lesions, as observed in the radiological features of S-DiPO. Five of the seven patients with S-DiPO had high-grade CiOP lesions, as shown in Fig. 5a,b (Patient 7; CiOP-G2) and Fig. 5d,e (Patient 12; CiOP-G1) (Table 2–3). In two of these patients (Patients 9 and 12), OP, CiOP, and ossified lesions were observed in close proximity within the same histological field (Fig. 5d,e). In contrast, the majority of patients with S-DiPO and Af had a nodular type (Patients 9, 24, and 31), displayed few or no bone marrow findings, and had smaller lesions (Fig. 6a–e, Patient 31; nodular type, maximum size-G0, bone marrow-G0) than those with I-DiPO (Fig. 6f, Patient 19; dendritic type, maximum size-G2, bone marrow-G3). The characteristics of the patients with I-DiPO and S-DiPO are summarised in Tables 2, 3 and Supplementary Tables S3 and S4.

## Discussion

In this study, we conducted a nationwide secondary survey to investigate the clinicopathological characteristics of patients with I-DiPO in Japan. We analysed the pathological features of 25 patients with DiPO (idiopathic, 18; secondary, 7) to understand the mechanism of ossification. I-DiPO predominantly exhibited a dendritic pattern. CiOP surrounding the ossification site was present in 71.4% (5/7) of the patients with S-DiPO and in 61.1% (11/18) of those with I-DiPO. These findings suggest that DiPO has a unique pathology characterised by a diffuse and notable transition to ossification through CiOP lesions.

Our data showed that I-DiPO and S-DiPO were more common in males than in females, which aligns with previous reports of non-Japanese patients[1–3,5,7,8,11,14,26,27]. However, patients with S-DiPO were older, had lesions randomly distributed throughout the lungs, and had a higher mortality rate than those with I-DiPO.

| Pathological type | Underlying diseases | No. of nodular type | No. of mixed type | No. of dendriform type | No. of dendriform type/all types | % | F test P value | |
|---|---|---|---|---|---|---|---|---|
| | Idiopathic | 0 | 5 | 13 | 13/18 | 72.2 | | |
| | Secondary-All | 2 | 2 | 3 | 3/7 | 42.8 | NS | |
| | Secondary-Af | 2 | 1 | 0 | 0/3 | 0 | < 0.05 | |

| Characteristic | Underlying diseases | No. of G0 | No. of G1 | No. of G2 | No. of G3 | No. of G2 + 3/all grades | % | F test P value |
|---|---|---|---|---|---|---|---|---|
| Ossification characteristic | | | | | | | | |
| With bone marrow grade | Idiopathic | 1 | 2 | 12 | 3 | 15/18 | 83.3 | |
| | Secondary-All | 2 | 2 | 2 | 1 | 3/7 | 42.8 | NS |
| | Secondary-Af | 2 | 1 | 0 | 0 | 0/3 | 0 | < 0.05 |
| Ossification MAX size grade | Idiopathic | 0 | 1 | 11 | 6 | 17/18 | 94.4 | |
| | Secondary-All | 1 | 2 | 2 | 2 | 4/7 | 57.1 | < 0.05 |
| | Secondary-Af | 2 | 1 | 0 | 0 | 0/3 | 0 | < 0.05 |
| Fibrosis | | | | | | | | |
| Subpleural fibrosis grade | Idiopathic | 17 | 1 | 0 | 0 | 0/18 | 0 | < 0.01 |
| | Secondary | | 2 | 3 | 2 | 5/7 | 71.4 | |
| OP grade | Idiopathic | 15 | 3 | 0 | 0 | 0/18 | 0 | < 0.05 |
| | Secondary | 2 | 2 | 0 | 3 | 3/7 | 42.8 | |
| Cicatricial OP (CiOP-grade) | Idiopathic | 1 | 6 | 9 | 2 | 11/18 | 61.1 | NS |
| | Secondary | 0 | 2 | 3 | 2 | 5/7 | 71.4 | |

**Table 3**. Comparison of the pathological characteristics between I-DiPO and S-DiPO by type and grading. *I-DiPO* idiopathic diffuse pulmonary ossification; *S-DiPO*, secondary diffuse pulmonary ossification; *NS,* not significant; *F test,* Fisher's exact test; Secondary-All, all S-DiPO cases; Secondary-Af, S-DiPO cases with atrial fibrillation [Af]; OP, organising pneumonia. Values indicate the number of cases. G0: grade 0, none; G1: mild; G2: moderate; G3: severe. To compare the pathological features between I-DiPO and S-DiPO, Fisher's exact test was used to evaluate the dendriform type. All other pathological parameters were expressed as a ratio of higher grades (number of patients with G2 and G3/number patients with all grades). Only patients with S-DiPO and atrial fibrillation were further compared with those with I-DiPO in terms of ossification characteristics (type, maximum size, and bone marrow component).

Conversely, patients in the I-DiPO group were younger and had more lesions in the lower lung fields, slower disease progression, and a lower mortality rate than those in the S-DiPO group. These differences suggest that idiopathic and secondary DiPO may have distinct pathogenic mechanisms. Histopathologically, subpleural pulmonary fibrosis and OP were more prevalent in patients with S-DiPO. Six of the seven patients with S-DiPO had a background of IP, unlike those with I-DiPO. In patients with idiopathic disease, no post-inflammatory signs or associated calcifications were evident. Ossification appeared distinct and unrelated to systemic ectopic bone formation or metabolic abnormalities. However, CiOP lesions were observed in both types of DiPO (approximately two-thirds of the patients). Therefore, the pathogenesis of DiPO may include CiOP lesions followed by ossification in both types of DiPO, indicating CiOP lesions as a shared pathological feature. These findings are consistent with those of recent studies, indicating that CiOP lesions are sometimes associated with ossification.

Moreover, OP, CiOP, and ossified lesions were observed in almost the same locations in the histopathological specimens from patients with S-DiPO. Similar to OP, the intraluminal distribution of ossified lesions as an air space of the alveoli was observed in some locations in I-DiPO, based on the findings of elastic fibre staining. These findings also suggest that, even in the absence of OP lesions in patients with I-DiPO, there may be a common pathophysiological factor in S-DiPO and I-DiPO, involving a transition from CiOP lesions to ossification.

In this study, CiOP lesions were frequently present in patients with both types of DiPO but they were not observed in the entire study cohort. Additionally, the nodular-predominant type of S-DiPO differed from the dendritic-type I-DiPO in terms of lesion size and the presence of bone marrow components (Table 3). Therefore, additional mechanisms beyond CiOP lesions may be involved in the pathogenesis of DiPO. The duration of bone formation may also affect the detectability or histological identification of CiOP lesions. Moreover, although CiOP lesions appear to contribute to the development of DiPO, the underlying causes of CiOP lesions and subsequent ossification remain unclear.

Heterotopic ossification (HO) is a pathological condition characterised by abnormal bone formation in soft tissues, such as muscles and joints. It primarily affects males and is typically triggered by trauma, surgery or rare genetic disorders. Although the precise mechanisms remain uncertain, fibroblast-like multipotent stem cells are thought to differentiate into osteoblasts under the influence of signals, such as from bone morphogenic protein and wingless-related integrated site/β-catenin, and various microenvironmental factors, including oxygen level, pH, and mechanical stress. Extracellular matrix (ECM) stiffness and male hormones have also been shown

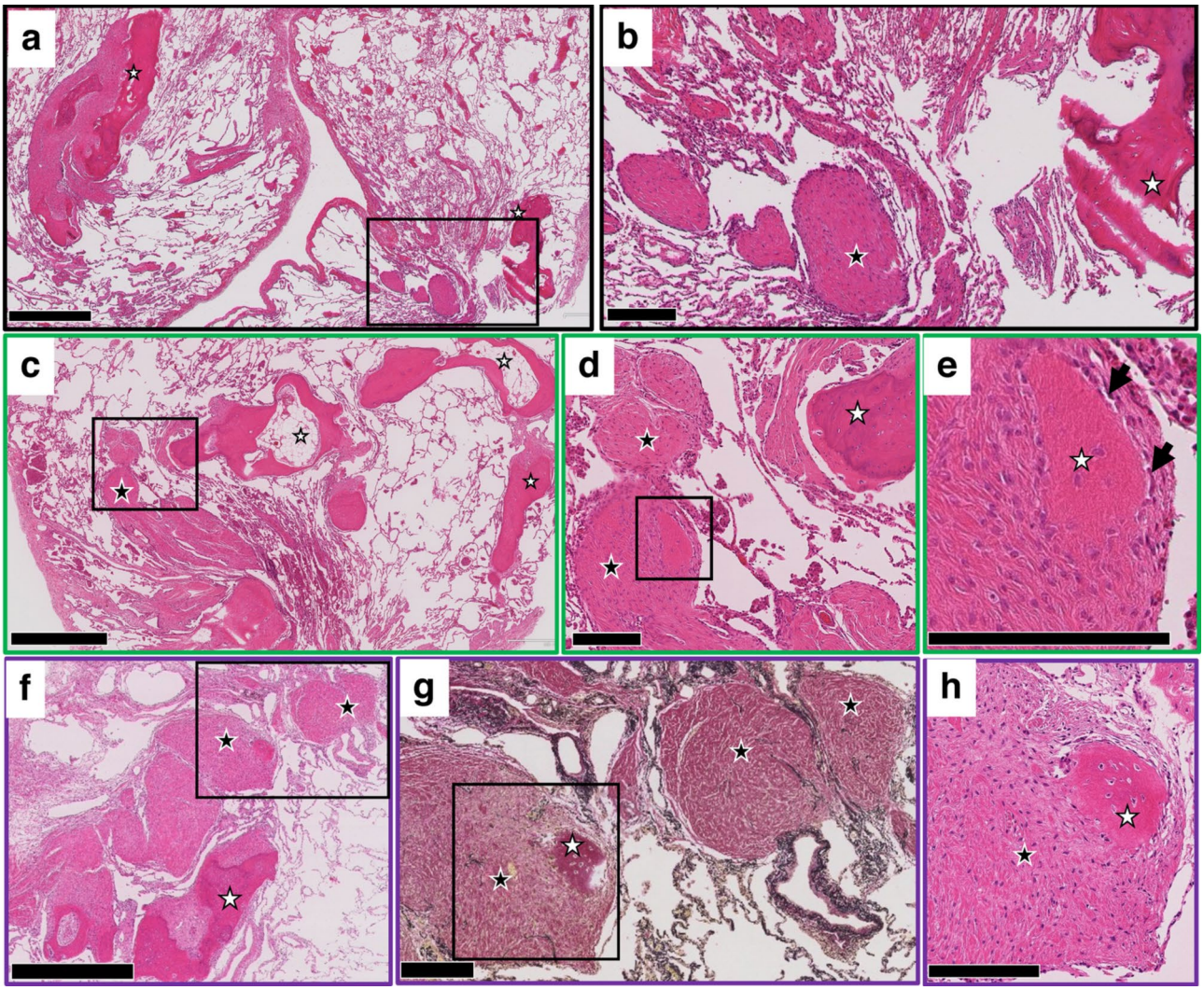


**Fig. 4**. Pathological findings of CiOP lesions in three patients with I-DiPO. (**a**) Low-power view of a specimen obtained from a patient with I-DiPO (Patient 37). Multiple foci of bone (white stars, maximum size-G1 and bone marrow-G1) were observed. (**b**) CiOP lesions (black star, CiOP-G2) observed close to ossified lesions (white star). High-magnification view of the area in the black rectangle in (**a**). (**c**) Low-power view of a specimen from a patient with I-DiPO (Patient 28). Multiple foci of bone (white stars, maximum size-G1 and bone marrow-G2) were randomly located. (**d**) CiOP lesions (black stars, CiOP -G2) observed close to ossified lesions (white stars). High-magnification view of the area in the black rectangle in (**c**). (**e**) Osteoblastic cells were occasionally observed in CiOP lesions with an ossified extracellular matrix (white stars). High-magnification views of the areas in the black rectangle in (**d**) and the black arrows in (**e**) indicate osteoblastic cells. (**f**, **g**) Low- and middle-power views of a specimen from a patient with I-DiPO (Patient 14). CiOP lesions (black stars, CiOP-G2) and ossified lesions (white stars, maximum size-G3) were observed in the alveolar spaces with elastic fibre staining of serial sections (haematoxylin and eosin and Elastica van Gieson staining). (**g**) High-magnification view of the area in black rectangle in (**f**). (**h**) The focus of the ossified lesion (white star) is visible within the CiOP lesion (black star). High-magnification view of the area indicated by the black rectangle in (**g**). Scale bars, 1 mm (**a**, **c**, and **f**) and 0.2 mm (**b**, **d**, **e**, **g**, and **h**). *CiOP* cicatricial organising pneumonia, *G* grade, *I-DiPO* idiopathic diffuse pulmonary ossification.

contribute to the ossification process[28–30]. CiOP has been frequently observed in late-stage COVID-19 patients, with lesions identified in the lungs. Moreover, heterotopic ossification post-COVID-19 has been documented in joints[31,32]. To the best of our knowledge, diffuse heterotopic ossification in the lungs has not yet been reported in post-COVID-19 patients. However, the frequent occurrence of CiOP suggests that the potential pulmonary ossification might emerge as a related finding in future investigations. Thus, the transition from fibrosis and scarring to ossification may represent a shared pathological process in both HO and DiPO, with ECM stiffness and male hormones potentially contributing to ossification as a part of a degenerative cascade. Given the rarity of DiPO, further studies, including genetic analyses, is warranted to elucidate its mechanisms, particularly in light of its higher prevalence of I-DiPO in younger patients.

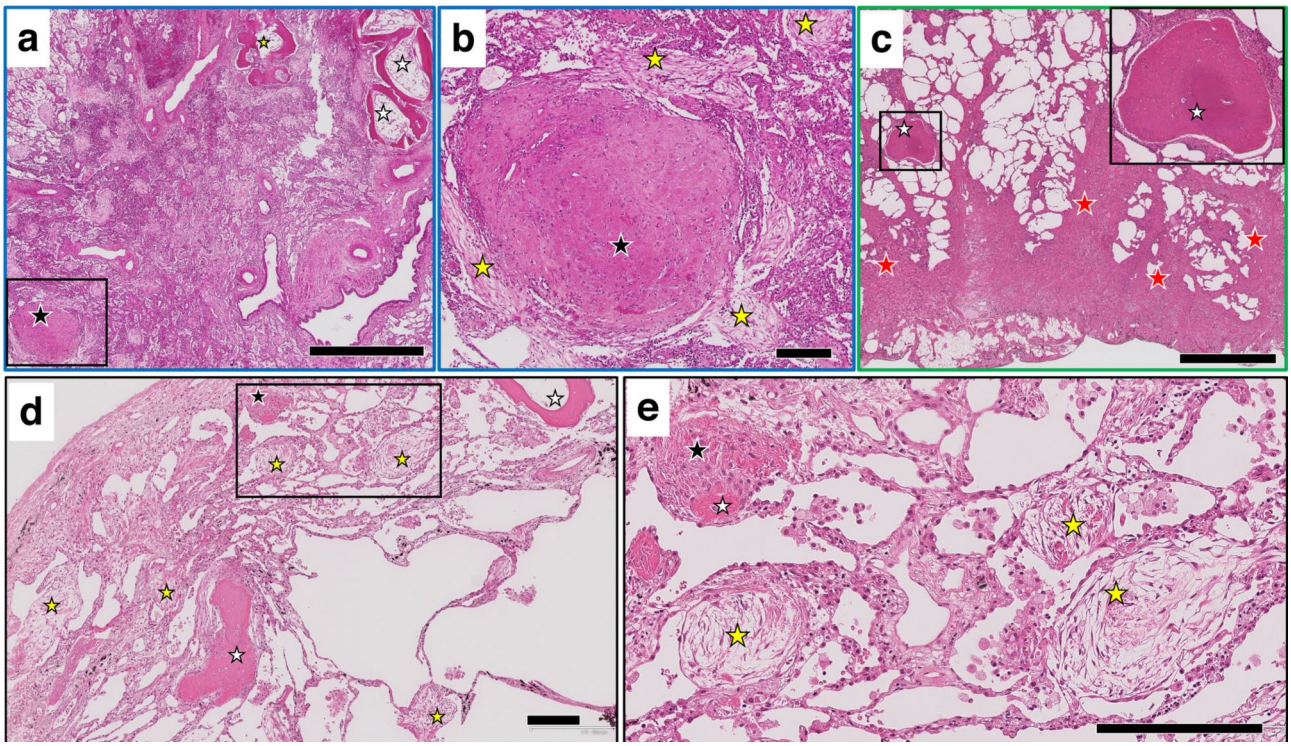


**Fig. 5**. Pathological findings of lung lesions in three patients with S-DiPO. (**a**) Medium-power view of a specimen from a patient with S-DiPO (Patient 7). Multiple foci of bone (white stars, mixed type, maximum size-G2, and bone marrow-G3) and a CiOP lesion (black star, CiOP-G2) are observed. (**b**) Notable OP findings (yellow stars, OP-G3) close to CiOP lesions. High-magnification view of the area indicated by the black rectangle in (**a**). (**c**) Low-power view of a specimen from a patient with S-DiPO (Patient 24). An ossified lesion (white stars, maximum size-G1, bone marrow-G0) with subpleural fibrosis (red stars, subpleural fibrosis-G3) is shown. Inset; High magnification view of the area in the black rectangle in (**c**). (**d**) Middle power view of a specimen from a patient with S-DiPO (Patient 12). (**d**, **e**) Various phases of the lesion, including OP (yellow stars, OP-G3), CiOP (black stars, CiOP-G1), and ossification (white stars, bone marrow-G0), observed in close proximity. e: High-magnification view of the black rectangle in (**d**). Scale bars: 2 mm (**c**), 1 mm (**a**), and 0.2 mm (**b**, **d**, and **e**). *CiOP* cicatricial organising pneumonia; DiPO, diffuse pulmonary ossification; G, grade; OP, organising pneumonia.

There were several limitations to this study. First, the small number of S-DiPO cases, along with a high mortality rate (three of seven patients), limited our ability to perform detailed comparisons of functional decline and disease progression. Second, post-mortem diagnoses for some patients with S-DiPO may introduce bias when comparing the survival rate with patients with I-DiPO, among whom no deaths were observed. Finally, the inclusion of only Japanese patients may limit the generalizability of our findings to broader populations. These limitations highlight the need for further studies with larger cohorts and extended follow-up periods to better understand the disease trajectory and prognostic factors in S-DiPO and I-DiPO.

Although the number of reports on patients with I-DiPO has been increasing annually, only a few studies have addressed patients with S-DiPO and the associated histopathological findings, and no previous study has reported presented a group of I-DiPO patients with adequate histopathological analysis including direct comparisons with S-DiPO. In this study, respiratory physicians, radiologists, and pathologists independently evaluated the clinical, radiological, and histopathological features of each patient. Therefore, these data, including histopathological findings from multiple patients from a nationwide survey of patients with DiPO, are valuable. This study included eighteen patients with I-DiPO and seven patients with S-DiPO, primarily those with IP or a cardiac conditions such as Af. Importantly, it is crucial to use patients with S-DiPO as a reference for evaluating patients with I-DiPO rather than focusing solely on the differences between these two types. Indeed, some findings differed between the groups, whereas others were common. These findings may provide useful insights into the pathogenesis of ectopic bone formation in the lungs.

Patients with DiPO appear to have a unique pathogenesis involving a diffuse and notable transition to ossification via CiOP lesions. This understanding may support the development of improved diagnostic strategies, and a broader understanding of heterotopic ossification as a pathological process.

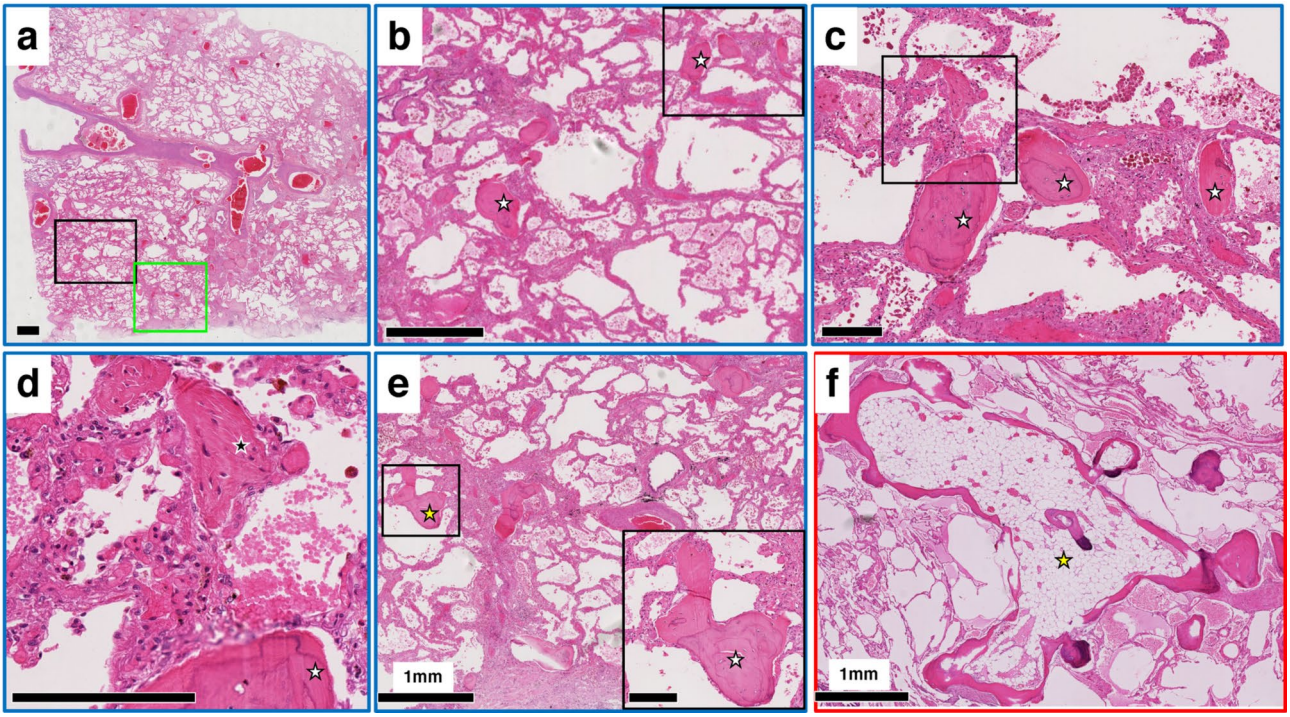


**Fig. 6**. Pathological findings of lung lesions from a patient with nodular-type S-DiPO and a patient with dendritic-type I-DiPO. (**a**–**e**) Several views of a specimen from a patient with nodular-type S-DiPO associated with AF (Patient 31). (**a**–**c**) Nodular-type DiPO lesions without bone marrow findings (white stars; bone marrow-G0). (**b**) High-magnification view of the black rectangle in (**a**). (**c**) High-magnification view of the area in the black rectangle in (**b**). (**d**) Small CiOP lesion (black star, CiOP-G1) close to the ossified lesion (white star). High-magnification view of the area in the black rectangle in (**c**). (**e**) Middle-power view of the same nodular-type S-DiPO (yellow stars, bone marrow-G0) showing a small, ossified lesion of approximately 0.5 mm in size (maximum size-G0). High-magnification view of the green rectangle in (**a**). Inset in (**e**); High-magnification view of the black rectangle in (**e**). f: Middle power view of a dendritic-type I-DiPO specimen (Patient 19) at the same magnification as in (**e**). Ossified lesion with bone marrow (yellow stars, bone marrow-G3) larger than 3 mm (maximum size-G2). Scale bars: 2 mm (**a**, **b**), 1 mm (**e**, **f**), and 0.2 mm (**c**, **d**, **e** inset). *CiOP* cicatricial organising pneumonia, *DiPO* diffuse pulmonary ossification, *G* grade.

## Data availability

The data supporting the findings of this study are available from the corresponding author upon request.

Received: 6 October 2024; Accepted: 20 March 2025
Published online: 11 April 2025

## References

1. Lara, J. F., Catroppo, J. F., Kim, D. U. & da Costa, D. Dendriform pulmonary ossification, a form of diffuse pulmonary ossification: A report of a 26-year autopsy experience. *Arch. Pathol. Lab. Med.* **129**, 348–353 (2005).
2. Konoglou, M. et al. Lung ossification: An orphan disease. *J. Thorac. Dis.* **5**, 101–104 (2013).
3. Peros-Golubicić, T. & Tekavec-Trkanjec, J. Diffuse pulmonary ossification: An unusual interstitial lung disease. *Curr. Opin. Pulm. Med.* **14**, 488–492 (2008).
4. Kanne, J. P., Godwin, J. D., Takasugi, J. E., Schmidt, R. A. & Stern, E. J. Diffuse pulmonary ossification. *J. Thorac. Imaging* **19**, 98–102 (2004).
5. Kim, T. S., Han, J., Chung, M. P., Chung, M. J. & Choi, Y. S. Disseminated dendriform pulmonary ossification associated with usual interstitial pneumonia: Incidence and thin-section CT-pathologic correlation. *Eur. Radiol.* **15**, 1581–1585 (2005).
6. Fernández-Bussy, S. et al. Dendriform pulmonary ossification. *Respir. Care.* **60**, e64–e67 (2015).
7. Tseung, J. & Duflou, J. Diffuse pulmonary ossification: An uncommon incidental autopsy finding. *Pathology* **38**, 45–48 (2006).
8. Egashira, R. et al. Diffuse pulmonary ossification in fibrosing interstitial lung diseases: Prevalence and associations. *Radiology* **284**, 255–263 (2017).
9. Mizushina, Y. et al. A rare case of asymptomatic diffuse pulmonary ossification detected during a routine health examination. *Intern. Med.* **51**, 2923–2927 (2012).
10. Nishioka, Y. et al. Nationwide retrospective observational study of idiopathic dendriform pulmonary ossification: Clinical features with a progressive phenotype. *BMJ Open Respir. Res.* **9**, e001337 (2022).
11. Gao, Y., Egan, A. M. & Moua, T. Dendriform pulmonary ossification complicated by recurrent spontaneous pneumothorax: Two case reports and a review of the literature. *Respir. Med. Case Rep.* **30**, 101067 (2020).
12. Kato, T., Ishikawa, K., Kadoya, M., Okamoto, K. & Kaji, M. Spontaneous pneumothorax in a patient with dendriform pulmonary ossification: A case report. *Surg. Today* **42**, 903–908 (2012).

13. Matsuo, H. et al. Progressive restrictive ventilatory impairment in idiopathic diffuse pulmonary ossification. *Intern. Med.* **57**, 1631–1636 (2018).
14. Carney, J. M., Mammarappallil, J. G., Sporn, T. A. & Pavlisko, E. N. Dendriform pulmonary ossification leading to bilateral lung transplant: A case report. *Virchows Arch.* **473**, 379–383 (2018).
15. Chan, E. D., Morales, D. V., Welsh, C. H., McDermott, M. T. & Schwarz, M. I. Calcium deposition with or without bone formation in the lung. *Am. J. Respir. Crit. Care Med.* **165**, 1654–1669 (2002).
16. Yousem, S. A. Cicatricial variant of cryptogenic organizing pneumonia. *Hum. Pathol.* **64**, 76–82 (2017).
17. Churg, A., Wright, J. L. & Bilawich, A. Cicatricial organising pneumonia mimicking a fibrosing interstitial pneumonia. *Histopathology* **72**, 846–854 (2018).
18. Woge, M. J., Ryu, J. H., Bartholmai, B. J. & Yi, E. S. Cicatricial organizing pneumonia: A clinicopathologic and radiologic study on a cohort diagnosed by surgical lung biopsy at a single institution. *Hum. Pathol.* **101**, 58–63 (2020).
19. Bin Saeedan, M., Farver, C., Mehta, A. C. & Yadav, R. Cicatricial organizing pneumonia with dendriform pulmonary ossification: An unusual cause for a recurrent pneumothorax. *Case Rep. Pulmonol.* **2019**, 2379145 (2019).
20. Travis, W. D. et al. An official American Thoracic Society/European Respiratory Society statement: Update of the international multidisciplinary classification of the idiopathic interstitial pneumonias. *Am. J. Respir. Crit. Care Med.* **188**, 733–748 (2013).
21. Kinoshita, Y., Mizuguchi, I., Hidaka, K., Ishii, H. & Watanabe, K. Familial diffuse pulmonary ossification: A possible genetic disorder. *Respir. Investig.* **55**, 79–82 (2017).
22. Edahiro, R. et al. Three cases of idiopathic diffuse pulmonary ossification. *Intern. Med.* **58**, 545–551 (2019).
23. Anan, K., Hisanaga, J., Kawamura, K. & Ichikado, K. Dendriform pulmonary ossification. *Intern. Med.* **58**, 1043–1044 (2019).
24. Enomoto, T. et al. Histologically proven dendriform pulmonary ossification: A five-case series. *Intern. Med.* **60**, 2261–2268 (2021).
25. Ono, K. et al. Case of idiopathic dendriform pulmonary ossification diagnosed by video-assisted thoracic surgery and followed over a long period of 12 years. *Ann. Jpn. Respir. Soc.* **2**, 246–268 (2003).
26. Whitaker, W., Black, A. & Warrack, A. J. Pulmonary ossification in patients with mitral stenosis. *J. Fac. Radiol.* **7**, 29–34 (1955).
27. Wilson, W. R., Sasaki, R. & Johnson, C. A. Disseminated nodular pulmonary ossification in patients with mitral stenosis. *Circulation* **19**, 323–331 (1959).
28. Li, J. X., Dang, Y. M., Liu, M. C., Gao, L. Q. & Lin, H. Fibroblasts in heterotopic ossification: Mechanisms and therapeutic targets. *Int. J. Biol. Sci.* **21**(2), 544–564 (2025).
29. Fu, L. et al. Fibroblasts mediate ectopic bone formation of calcium phosphate ceramics. *Materials (Basel).* **15**(7), 2569 (2022).
30. Hwang, J. H. et al. Extracellular matrix stiffness regulates osteogenic differentiation through MAPK activation. *PLoS ONE* **10**(8), e0135519 (2015).
31. Chaitani, H., Fabeck, L. & Koulischer, S. Heterotopic ossification following COVID-19 infections: Systematic literature review of case reports and case series. *BMC Musculoskelet. Disord.* **25**(1), 421 (2024).
32. Roden, A. C. et al. Late complications of COVID-19. *Arch. Pathol. Lab. Med.* **146**(7), 791–804 (2022).

## Acknowledgements
We thank Arimi Ishikawa and Naomi Kuwahara for their technical assistance. We also like to thank Editage for providing excellent editing assistance.

## Author contributions
Y.T., Y.N., Y.K., Y.T., A.H., T.J., and R.E. participated in the conception, hypothesis delineation, study design, clinical and experimental work, data analysis, and manuscript preparation. T.H., M.M., T.B., Y.F., M.K., K.I., Y.I., S.I., Y.H., T.H., K.H., S.H., C.H., T.K., M.O., and M.Y. participated in the clinical work. M.T. and T.S. reviewed and approved the manuscript and took responsibility for its content.

## Funding
This study was supported in part by a Grant-in-Aid for Scientific Research from the Ministry of Education, Culture, Sports, Science and Technology (MAXT), Japan. It was also partially supported by a grant from the Diffuse Lung Diseases Research Group of the Ministry of Health, Labour, and Welfare of Japan.

## Declarations

## Competing interests
The authors declare no competing interests.

## Research involving human participants
This study was conducted in accordance with the Declaration of Helsinki and was approved by the Institutional Ethics Committee of Nippon Medical School (approval number: O-2021-033 [2022-178, 13 July 2022]).

## Informed consent
Informed consent was obtained from all living individual participants included in the study. For deceased individuals, consent for the use of their tissues in research was obtained from their next of kin or legal representatives. All procedures followed were in strict accordance with the ethical standards of the responsible committee on human experimentation.

## Additional information
**Supplementary Information** The online version contains supplementary material available at https://doi.org/10.1038/s41598-025-95307-0.

**Correspondence** and requests for materials should be addressed to Y.T.